COLORADO

Department of Transportation

CDOT Office of Applied Research

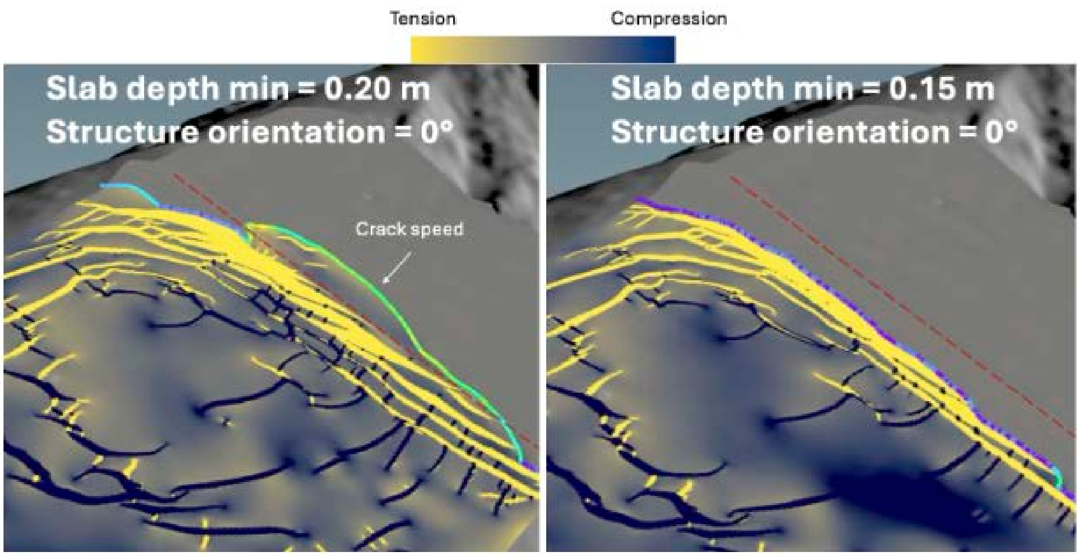

A Numerical Study of the Feasibility of Vertical Avalanche Defense Structures

Francis Meloche PhD

April 2026

CDOT Report Number: CDOT-2026-01

Technical Report Documentation Page

1. Report No.	2. Government Accession No.	3. Recipient's Catalog No.
CDOT-2026-01		

4. Title and Subtitle	5. Report Date
A Numerical Study of the Feasibility of Vertical Avalanche Defense Structures	April 2026
	6. Performing Organization Code
7. Author(s) Francis Meloch PhD Co-Authors: Ron Simenhois, Don Sharaf, Johan Gaume PhD, and Ethan Greene	8. Performing Organization Report No.
9. Performing Organization Name and Address David Hamre and Associates, LLC PO Box 111492 Anchorage, AK 99511	10. Work Unit No. (TRAIS) 11. Contract or Grant No. PO 411041516
12. Sponsoring Agency Name and Address Colorado Department of Transportation Office of Applied Research 2829 W. Howard Place Denver, CO 80204	13. Type of Report and Period Covered Final Report (2025-26) 14. Sponsoring Agency Code

15. Supplementary Notes

Prepared in cooperation with PooledFund.org, TPF 5(497) - Transportation Avalanche Research Pool (TARP)
Collaborators: Ron Simenhois, Don Sharaf, Johan Gaume, & Ethan Greene PhD

16. Abstract

Traditional avalanche defense structures are costly to install and maintain, visually intrusive, and must be placed perpendicular to slopes. Many highway avalanche programs, therefore, rely on active measures like explosives, which carry inherent risks and may not prevent all large avalanches from reaching roadways. This project investigates an innovative alternative: vertical, downslope-oriented structures designed to arrest avalanche crack propagation at a fraction of the cost and visual impact.

Using over 300 numerical simulations, this study demonstrated the technical feasibility of vertical avalanche defense structures. The advanced depth-averaged Material-Point Method model—validated specifically for snow avalanches—examined crack propagation dynamics across simple slopes, complex analytical terrain, and real-world topography (Stanley Path, Colorado).

17. Keywords	18. Distribution Statement
Avalanche, Avalanche Defense Structure, Fracture Propagation, Fracture Arrest, Stanley Slide Path	This document is available on CDOT's website: https://www.codot.gov/programs/research

19. Security Classif. (of this report)	20. Security Classif. (of this page)	21. No. of Pages	22. Price
		34	

Form DOT F 1700.7 (8-72) Reproduction of completed page authorized

Final Technical Report - TARP Avalanche Defence Structures

A Numerical Study of the Feasibility of Vertical Avalanche Defense Structures

Main investigator: Francis Meloche

Collaborators: Ron Simenhois, Don Sharaf, Johan Gaume, & Ethan Greene

March 25, 2026

Executive Summary

The Challenge

Traditional avalanche defense structures are costly to install and maintain, visually intrusive, and must be placed perpendicular to slopes. Many highway avalanche programs, therefore, rely on active measures like explosives, which carry inherent risks and may not prevent all large avalanches from reaching roadways. This project investigates an innovative alternative: vertical, downslope-oriented structures designed to arrest avalanche crack propagation at a fraction of the cost and visual impact.

Scientific Verification Results

Using over 300 numerical simulations, this study demonstrated the technical feasibility of vertical avalanche defense structures. The advanced depth-averaged Material-Point Method model—validated specifically for snow avalanches—examined crack propagation dynamics across simple slopes, complex analytical terrain, and real-world topography (Stanley Path, Colorado).

Key Findings

Effectiveness Confirmed: Structures successfully arrested crack propagation when designed according to specific geometric and snow depth parameters. The primary mechanism is slab thickness reduction over the structure, promoting tensile fractures that halt avalanche development.

Clear Design Parameters: Critical thresholds were identified: (1) Minimum structure ratio (height/width) of 0.5 for buried structures; (2) Maximum snow burial depth of 0.15–0.30 m depending on snow density (maritime vs. continental climates); (3) Minimum width of ~0.6 m for unburied structures; (4) Downslope length extending to slopes ≤27° (snow friction angle).

Layout Optimization: Structure orientation and positioning matter. Downslope orientations (0° to 10° from slope-parallel) performed best, while orientations approaching cross-slope configurations (>20°) deviated from the core concept. Discontinued structures (mimicking natural obstacles) require precise spacing (~6 m) aligned with super-shear critical crack length.

Real-World Validation: Simulations on Stanley Path terrain, incorporating realistic snow distribution patterns from wind loading, confirmed that structures can arrest avalanches in complex topography when properly dimensioned and positioned between existing avalanche control systems.

Recommendation for Future Phases

The numerical modeling phase has established robust scientific foundations and design guidelines. The next critical step is advancing to structural engineering and field validation. Phase 2 should focus on:

- **Structural Design Engineering:** Collaborate with geotechnical engineers specializing in alpine environments to develop structures that emerge from snowpack, resist wind loading, and withstand multi-year snow stress cycles. Incorporate 3D wind-field modeling to predict snow burial patterns.
- **Prototype Development:** Design lightweight, dual-wall configurations that maintain required width (≥0.6 m) while minimizing material use. Consider both earth-structures (gabions) and metal stand-alone designs based on installation logistics and environmental durability.
- **Field Implementation:** Deploy prototype at Stanley Path, Colorado, leveraging existing Remote Avalanche Control Systems infrastructure. Monitor performance through multiple winter seasons to validate snow mechanics predictions and refine design parameters.
- **Validation Simulations:** If needed, conduct additional numerical simulations with finalized structural designs to confirm crack arrest effectiveness under realistic burial and loading scenarios.

Conclusion

The scientific verification phase has successfully established that downslope vertical avalanche defense structures can arrest weak-layer crack propagation and limit avalanche size. With clear design parameters validated across 300+ simulations and real-world terrain analysis, the project is ready to advance to engineering design and field testing.

1.0 Introduction

1.1. Background

Avalanche defense structures in starting zones stabilise seasonal snow and help prevent avalanches. Traditionally, large structures are placed perpendicular to the slope to achieve this effect. However, this approach has significant drawbacks: installation and maintenance are costly, and the structures have a strong visual impact. As a result, many highway avalanche mitigation programmes rely on active measures, such as explosives, to reduce avalanche risk. While effective, these methods carry inherent risks to personnel and may not always prevent large avalanches from reaching roadways.

This study investigates the potential of vertical avalanche defense structures to protect transportation corridors from large avalanches. These structures could offer a more cost-effective solution with a lower visual impact. Using newly developed numerical simulations of avalanche release, this work aims to evaluate and quantify the effectiveness of different design strategies, including variations in size, height, length, and layout.

1.2. Avalanche propagation and crack arrest

Dry-snow slab avalanche release is a multiscale mechanical process that starts with microstructural damage to the snow crystals that constitute a weak layer underneath a cohesive snow slab (McClung D. & Schaerer P., 2006; Schweizer et al., 2003). This damage can form a crack in the weak layer, and if the length of this crack is long enough, sustained dynamic crack propagation will occur along the slope. The dynamic crack propagation essentially breaks the weak layer, causing the slab above to lose support and start to move downslope (due to gravity) (Gaume et al., 2014; Heierli et al., 2008). Tensile stress in the slab will build up until the tensile stress reaches the tensile strength of the slab (Sigrist & Schweizer, 2007). When the stress exceeds the strength, the slab will fracture perpendicularly to the weak layer, and in some cases, it will cause the crack propagation to stop. Recent studies investigate the influence of slab tensile fractures causing crack propagation to stop; however, not all fractures can cause an arrest, and a significant "slow-down" of the crack speed was necessary (Meloche et al., 2025; Trottet et al., 2022). They also investigate the crack arrest mechanism for large avalanches, where crack propagation speed is very high in the downslope direction. However, crack speed is lower in the cross-slope direction, which could make it easier to stop in that direction. Considering the interaction between the crack speed and the slab fracture leading to crack arrest, this work investigates the feasibility of a cross-slope structure capable of stopping the propagation and limiting the avalanche size.

1.3. Model set-up

To investigate the feasibility of this potential structure, we used a simulation method to model crack propagation in snow, using a depth-averaged Material-Point Method (DAMPM). This method was developed and validated specifically for snow avalanches by Guillet et al. (2023) and was used by Meloche et al. (2025) to study crack arrest in snow avalanches. For all the details about the method itself, the validation and the parameterization, please consult Guillet et al. (2023) and Meloche et al. (2025). With this method, our main goal is to examine the two primary objectives of the structure, which are 1) to emerge from snow to prohibit crack propagation, and 2) if submerged, to reduce the slab thickness and promote slab fracture. All tested parameters are listed in *Table 1*, we presented a key summary for every simulation related to objective 1 in *Table 2*, as well as for objective 2 in *Table 3*.

Table 1. List of all variables, including their names, symbols, and descriptions.

Variable	**Description**	**Variable**	**Description**
ρ	Slab density	τ_p	Weak layer shear strength
ρ_0	Initial slab density	τ_g	Gravitational shear stress
σ_t	Slab tensile strength	L_{wl}	Weak layer intact length or area
H_{slab}	Slab depth	Λ	Characteristic elastic length
W_{wall}	Wall width	H_{length}	Slab depth reduction length
H_{wall}	Wall height	S_{asym}	Cross-loading asymmetric parameter
K_{wall}	Wall stiffness	θ	Slope angle
a_{sc}	Super shear critical length	ϕ	Internal snow friction angle

1.3.1. Unburied structure

An unburied structure should effectively stop crack propagation because there is no material (snow slab) to transmit the stress wave above the structure. However, a flexible structure could potentially disrupt the weak layer on the side. We model a simple wall to test the propagation through an unburied structure with different stiffness. This should provide a minimum width and stiffness (in relation to snow stiffness) for the potential structure (*Table 2*). These simulations assumed that the snow slab is **attached** to the structure and could transmit stress through it. This assumption is unlikely in continental and intermountain snowpack, where faceting is likely to develop around these structures. However, this unlikely scenario was still assessed in our simulations to account for maritime climates where snow might refreeze or settle heavily around the structure. <u>In the situation that the slab is not “attached” to the unburied structure (most likely), then the structure should be effective in stopping the propagation cross-slope.</u>

Table 2. Key summary of the model parameters and values for the simulation ***<u>with no weak layer (infinite strength) or unburied structure with no slab on top.</u>*** *The most important parameters for which a sensitivity analysis was conducted are highlighted for each type of simulation. At the end of the table, the key objectives of each simulation type are presented, along with the section and figure in which the results are displayed.*

No weak layer or Unburied structure			
Parameters/Simulation	Planar slope 30 by 10 m	Long bowl 80 by 120 m	Discontinued structure 80 by 120 m
ρ_0 Initial slab density	60 to 100 kg m^{-3}	80 kg m^{-3}	80 kg m^{-3}
H_{slab} Slab depth	0.5 m and no slab on the structure	**0.5 m**	0.5 m and no slab on structure
ρ Slab density	Figure 1a	Figure 1a	Figure 1a
σ_t Slab tensile strength	Figure 1a	Figure 1a	Figure 1a
W_{wall} Wall width	**0.3 to 1.3 m**	**0.15 m to 2 m**	9 m
H_{wall} Wall height	NA	0.1 m	1-3 m
Spacing structure	NA	NA	**1 to 10 m**
τ_p^{wall} Wall weak layer strength	Infinite strength	Infinite strength	Infinite strength
Key objectives of the simulation	**Minimum width wall with no slab on top.**	**Minimum width with slab on top, but no weak layer.**	**Minimum spacing between structure.**
Results presentation	**Section 2.1 Figure 3**	**Section 2.3.1 Figure 6**	**Section 2.4 Figure 10-11**

1.3.2. Buried structure

In the case that the structure is buried, the objective of the structure would be to reduce the slab depth/thickness to promote slab fractures, hopefully causing a crack arrest. To replicate this, the mechanical properties of the slab (slab density and tensile strength) were parameterized in relation to the slab depth (Figure 1-b). These parameterizations are based on extended cold lab measurements by Sigrist (2006) and McClung (2009), which are considered reliable for snow mechanical properties in the snow mechanics community. First, the slab density is parameterized using the slab depth and the empirical power-law fit of McClung (2009). His empirical fit uses an initial density of 100 kg m^{-3} and was fitted to his study data; however, the initial density can be adjusted to fit different snow climates, such as continental (lower densities) or maritime (higher densities), as found in coastal Alaska. We tested three different initial densities (Figure 1-b) to find a relation that would enable us to extrapolate to other initial density values in the future if needed (Table 3).

Table 3. Key summary of the model parameters and values for the simulation ***with a weak layer and buried structure with a slab on top.*** *The most important parameters for which a sensitivity analysis was made are highlighted for each type of simulation. At the end of the table, the key objectives of the simulation type are presented, as well the section and the figure in which are presented the results.*

Buried structure **(with weak layer)**				
Variables	Planar slope 30 by 10 m	Long bowl 80 by 120 m	Long bowl 80 by 120 m	Stanley Path 100 by 150 m
ρ_0 Initial slab density	**60 to 100 kg m^{-3}**	80 kg m^{-3}	80 kg m^{-3}	80 kg m^{-3}
H_{slab} Slab depth	**0.1 to 0.5 m**	**0.5 m**	0.5 m	**0.15 to 0.35 m**
ρ Slab density	Figure 1a	Figure 1a	Figure 1a	Figure 1a
σ_t Slab tensile strength	Figure 1a	Figure 1a	Figure 1a	Figure 1a
W_{wall} Wall width	2 to 15 m	**6 – 10 m**	9 m	9 m
H_{wall} Wall height	0.5 – 1 m	1 – 3 m	1-3 m	2-3-4 m
Length structure	10 m (full slope)	120 m (full slope)	**40 to 120 m**	120 m (full slope)
Structure orientation	0 ° (y-axis)	0 ° (y-axis)	0 ° (y-axis)	**-30° to 20° (y-axis)**
τ_p^{wall} Wall weak layer strength	1 kPa	1 kPa	1 kPa	1 kPa
Key objectives of the simulation	**Minimum slab depth covering the structure and initial density.**	**Minimum slab depth covering the structure (bigger slope).**	**Minimum length of the structure.**	**Minimum slab depth and structure orientation.**
Results presentation	**Section 2.1 Figure 4-5**	**Section 2.3.2 Figure 7**	**Section 2.3.3 Figure 8-9**	**Section 3 Figure 12-13**

The structure was modeled as a ridge-like feature with a smooth angle (Gaussian). The reason behind this choice of "smooth structure" is to replicate the smoothing of the structure being buried by snow throughout the season. Even if the structure on the ground is triangular with "sharp edges", the burial of the structure by the snowfall will result in smoother edges and angles, as the structure is being buried. Our numerical model can only replicate the top part of the unstable snowpack, with the slab and the weak layer on top of a simulated terrain. **In other words, our model doesn't replicate, for example, 2-meter of snowpack on top of the structure, but only the 50 cm unstable slab on top of it.**

We also tested three different simulation geometries of terrain, ranging from a simple planar slope to a truly complex topography. The first geometry was a simple linear slope where we tested only the cross-slope propagation (Figure 1-a). The second simulation geometry was a long analytical bowl shape measuring 80 m wide by 120 m long (Figure 1-d). This geometry was used to avoid boundary effects in the simulation while replicating a realistic avalanche starting zone. The third and final geometry is the Stanley Path in Colorado, above Highway 40. Avalanche simulations were initialised in a location where a GazEx exploder is installed over an area of 100 m by 150 m, and the added structure is located between Gasex positions 1 and 2 (Figure 1-c). All types of simulations and relevant parameters are summarized in *Table 2* and *Table 3*. We also include in *Table 2* and *Table 3*, the main objective of each type of simulation, as well as the sections and figures in which the results are presented.

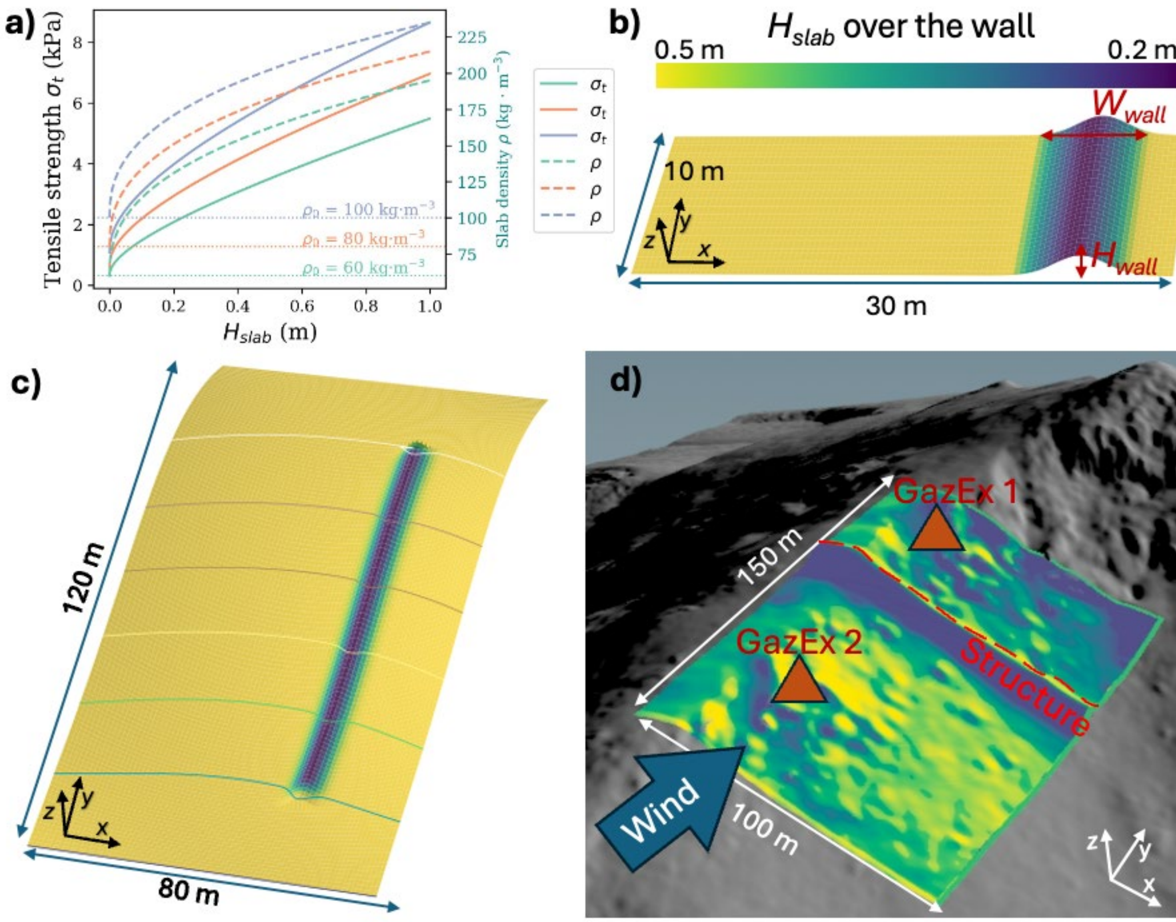

Figure 1. Geometry simulation and slab depth parameterization. a) Slab depth parameterization using Sigrist (2006). b) Cross-slope simulation with a Gaussian-shaped structure c) Long-bowl simulation d) Complex terrain simulation on Stanley Path. The colormap for the slab depth values is defined in a).

1.3.3. Discontinued unburied structure

In addition to a simple linear structure, we tested a single linear discontinued structure and two "offset" discontinued structures (*Figure 2*). The idea was to replicate unburied obstacles, such as trees and rocks, to promote crack arrest. Several parameters were tested, such as the structure length, taper length, and structure spacing.

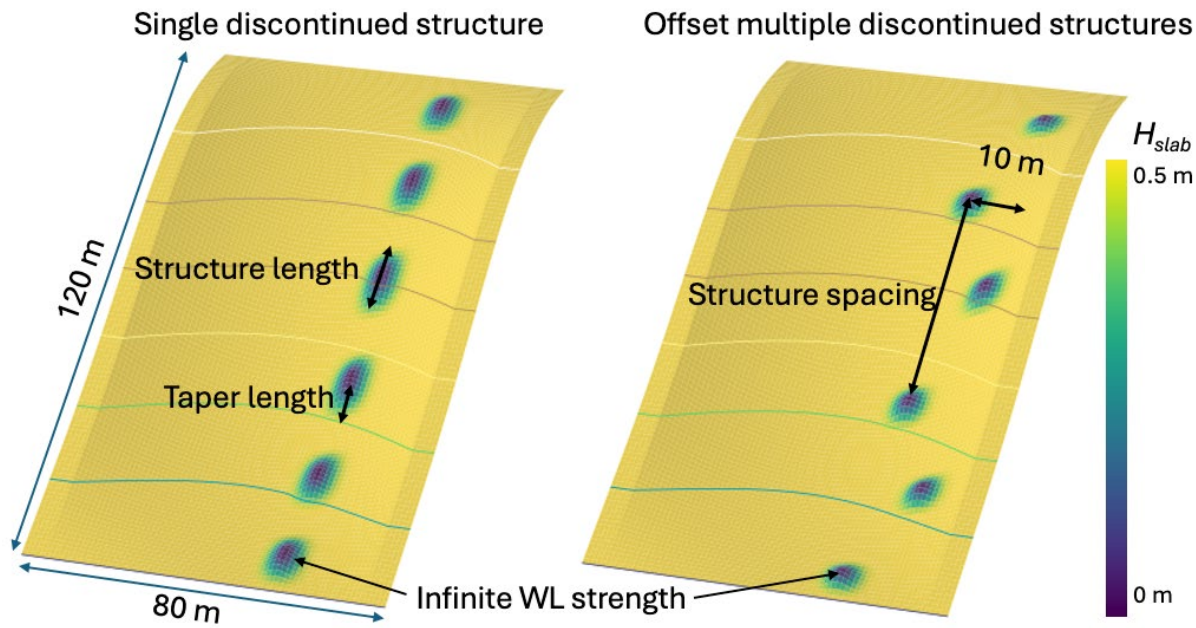

Figure 2. Discontinued unburied structure, with a single discontinued structure (left) and two offset discontinued structures (right). These structures are unburied, parameterized with a zero-slab depth and an infinite weak layer strength.

2. Evaluation of vertical designs using numerical simulations

2.1. Unburied structure with an attached slab

We tested several parameters for the unburied structure, namely the structure stiffness (K_{wall}), structure width (W_{wall}), characteristic length (Λ), and slab tensile strength (σ_t). In this context, the characteristic elastic length (Λ) of the system (slab and weak layer) is a measure of how far the effect of a crack or collapse in a weak snow layer spreads through the slab's elastic redistribution[1], meaning that the shear stress in the weak layer can be "felt" in front of the crack through slab elastic redistribution. It can indicate the length of the influence of the crack (Gaume et al., 2013, 2014), **thus an important length for determining the width of the potential structure.** The resulting variable from the simulation is the intact length of the weak layer on the other side of the structure, Intact length L_{wl}. We show a scaling of our simulations with the four parameters named above, and the results are well distinguished between propagation across the structure or not (*Figure 3*). An important distinction here is

[1] Due to elasticity of the slab and of the weak layer, the disturbance induced by the crack is felt ahead of the crack tip, at a distance related to this characteristic elastic length Λ.

to note that the slab and the particle representing the structure had the same elastic modulus during these simulations.

<u>Lay summary 2.1</u>: The minimum width of the wall should be at least 0.6 m to stop crack propagation, for cases where the structure is unburied and stress waves are transmitted through the structure.

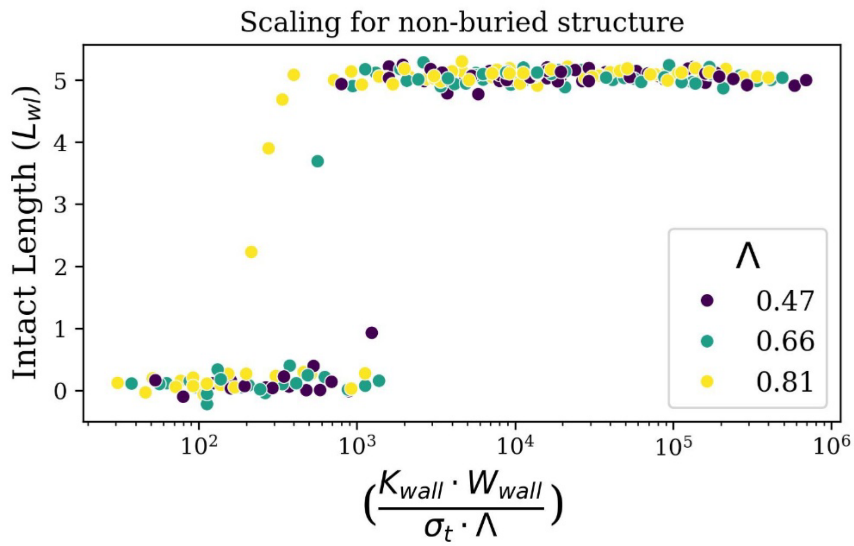

Figure 3. ***Scaling of the weak layer intact length for an unburied structure as a function of wall stiffness relative to snow properties.*** *The intact length L_{wl} transitions from near zero to a saturated regime with increasing nondimensional scaling indicating the threshold at which the structure becomes wide and stiff enough to prevent cracks from propagating across it and causing avalanches across the entire slope. Variations in Λ values have a limited effect on crack propagation over the structure relative to the structure geometry, with the data collapsing onto a common trend, <u>suggesting that similar unburied structure designs are expected to perform comparably across a range of snowpack conditions within the modeled parameter space.</u>*

2.2. Simple planar slope with buried structure

To explore different possible dimensions of a buried structure, we first investigate these dimensions using a simple planar slope with a ridge-like structure and a slab depth reduction. We tested several parameters with over 800 simulations: Slab depth over the wall H_{slab}, Wall width W_{wall}, Wall height H_{wall}, Slab length reduction H_{length}, Slab Asymmetric loading S_{asym} (mimicking cross-slope wind loading), and the initial density of the slab parameterization ρ_0. We computed a partial dependence analysis of their importance in distinguishing between an arrest or a propagation. The contribution of each variable can be approximated only by how much dependence they explain, like a steep line for a significant dependence and a flat line not very significant. This analysis serves as exploratory analysis to identify the most important variable. *Figure 4* shows that the slab depth over the wall and the initial density are the most important variable to distinguish between an arrest and a propagation. The rest of the variables seems to have less important effect compared to the other two above.

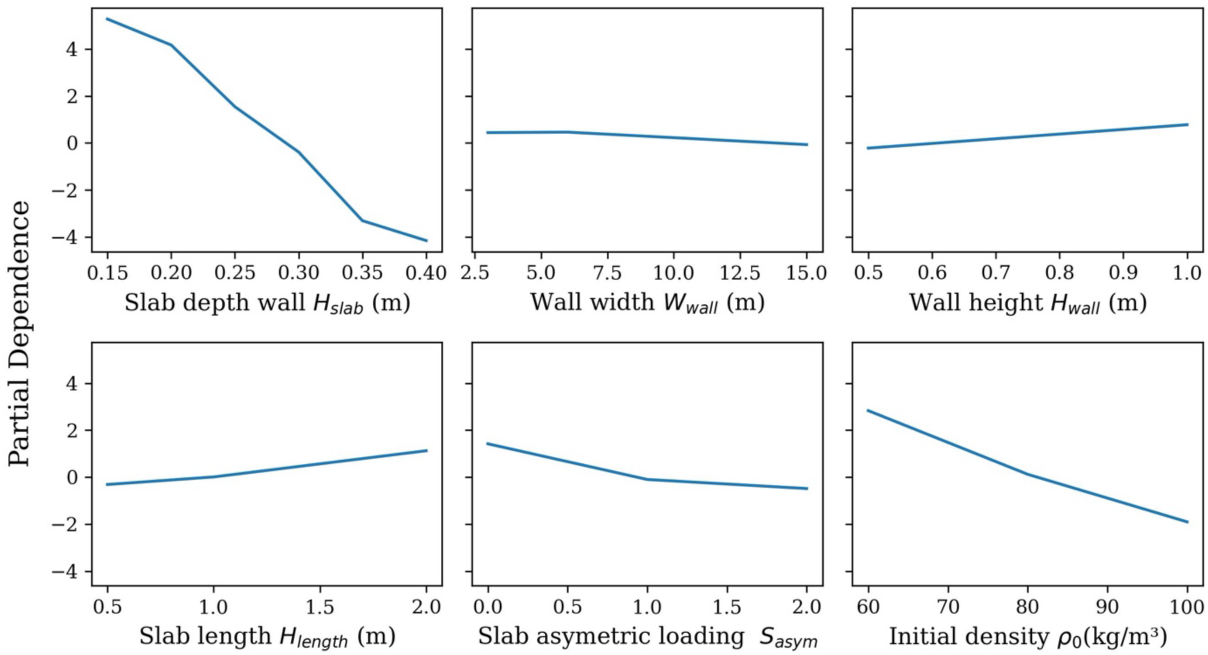

Figure 4. Partial dependence analysis on the preliminary simple planar slope simulations.

Figure 5-a shows the resulting intact weak layer lengths with three different initial densities (ρ_0) (*Figure 1*-b), and the slab depth covering the wall. The distinction between an intact weak layer length across the structure (value around 5) and 0 (no intact weak layer left), for different values of slab depth covering the structure depends highly on the initial density, and the curve is shifted as the initial density increases (see Figure 5-1). Now, there is no clear value of slab depth that perfectly distinguishes between arrest and propagation, and the secondary variables, mostly structure dimensions, still have an effect that explains the residual variability in simulations.

Figure 5-b shows a scaling with all the variables tested, but a lot of variability exists as not all the relations between variables can be explained. It is also important to note that variability in the results was observed because of the boundary effect of a small planar slope.

<u>Lay summary 2.2</u>: The most important parameter for the buried structure scenario to distinguish between an arrest or a propagation is the slab depth covering the structure. The minimum slab depth varied between 0.15 and 0.3 depending on the initial density.

In other words, thicker stronger slabs above 150 kg m^{-3} of density and 4 kPa of tensile strength, will allow propagation across the structure.

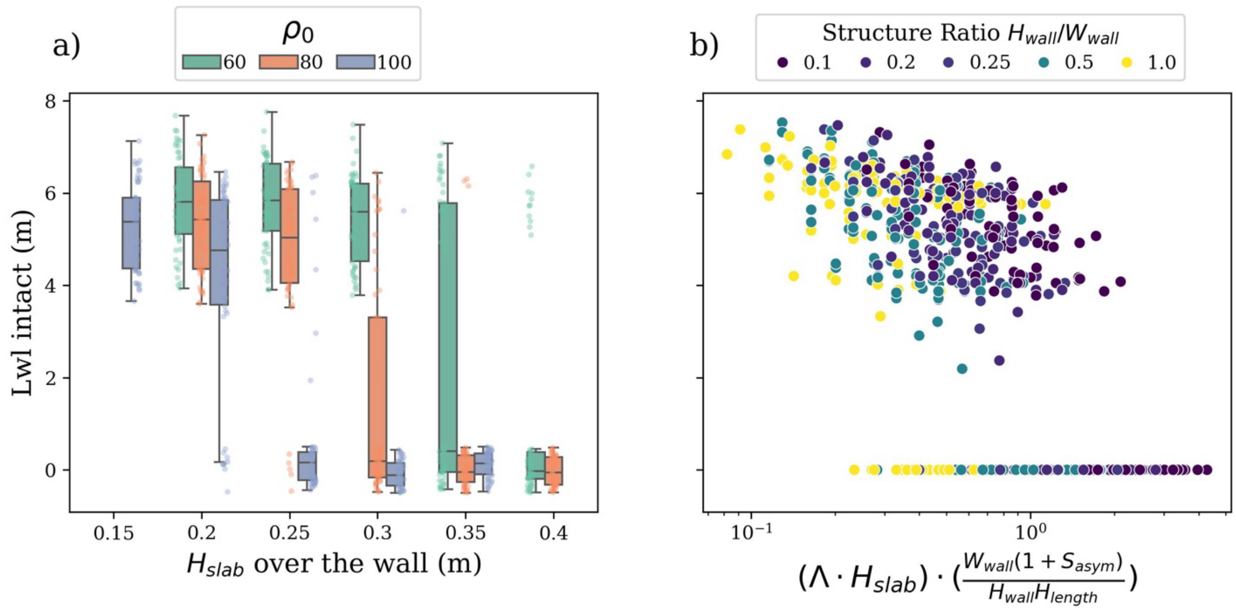

Figure 5. ***Numerical results showing the effectiveness of a buried cross-slope structure in arresting weak-layer crack propagation.*** *(a) Intact weak-layer length ($L_{wl,intact}$) versus slab depth above the structure (H_{slab}) for different initial snow densities (ρ_0). High values indicate successful crack arrest; $L_{wl,intact} = 0$ indicates full propagation. A clear, density-dependent threshold is observed: denser slabs fail at shallower burial depths, consistent with stronger slabs bridging the structure.* ***(b)*** *Scaling of $L_{wl,intact}$ using a dimensionless parameter combining slab load and structure geometry. Colors indicate structure aspect ratio (H_{wall}/W_{wall}). Taller, narrower structures are more effective at arresting cracks, while shorter, wider structures fail more readily. The scaling captures the overall trend but exhibits substantial scatter. This shows that the structure's effectiveness strongly depends on slab density and structure geometry.*

2.3. Long-bowl simulation with buried structure

In the simple planar slope simulations, we observed some boundary effects in the simulation that could affect the results of a few simulations. In addition, we also wanted to investigate the full steady-state crack propagation speed in both the cross-slope and down-slope directions simultaneously. These simulations require more memory and computing time, so fewer simulations were possible. The long-bowl simulation geometry allows us to investigate additional parameters, such as different layout positions in the starting zone, including the distance to trigger, structure length, and the arrangement of multiple smaller structures.

2.3.1. Stress wave through the slab

First, we investigated the case where a structure was buried but with no weak layer (infinite strength) and validated if a stress wave could be transmitted in the slab above the structure. These simulations enabled us to approximate the minimal width of the structure in case no weak layer is present on the structure, but stress wave could still transmit through the slab and propagate on the other side of the structure. *Figure 6* shows the residual broken weak layer length beyond the structure with different structure width. When the structure width is near 0.5 m or larger, the stress wave in the slab is not enough to transmit beyond the structure and break the weak layer. However, with a structure width around 0.3 m, the stress wave is transmitted through the slab and can lead to weak layer failure to some extent, producing a crack length beyond the wall of around 2-3 m, but was not sufficient to continue the crack propagation in our shear-based model. Our model only reproduces shear-based propagation, but in reality, a crack length of this order is sufficient to start the collapse-based propagation (anticrack) before transitioning again to shear-based (Trottet et al. 2022).

<u>Lay summary 2.3.1</u>: Numerical simulations suggest that the buried structure needs to be at least 0.6 m wide to prevent the least amount of broken weak layer on the other side of the structure. This will inhibit the propagation from restarting on the other side.

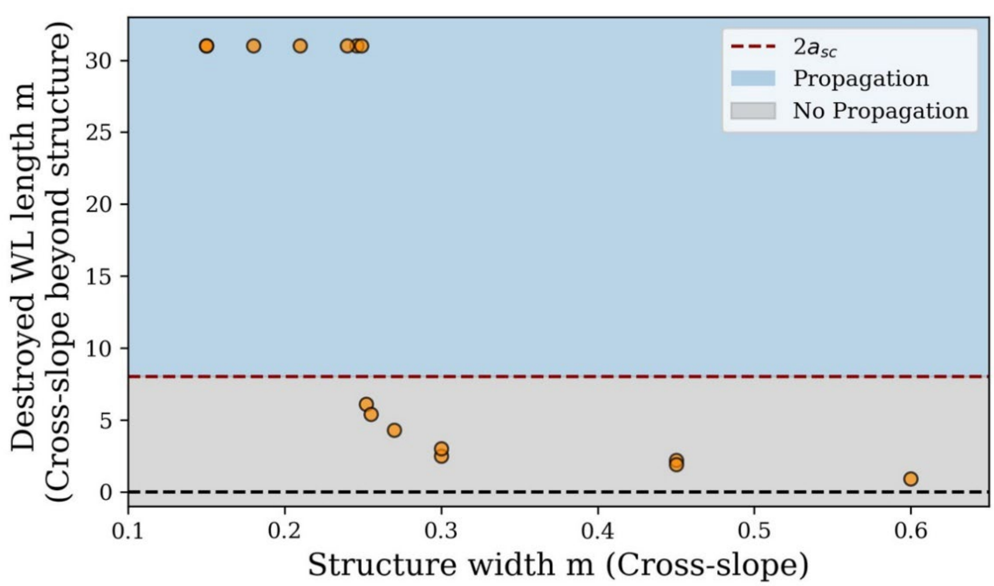

Figure 6. Simulations with a slab on top of the structure, but with no weak layer (infinite strength). The x-axis represents the width of the structure, and the y-axis represents the cross-slope length of broken weak layer beyond the structure. The red dotted lines represent

$2a_{sc}$, *which is the super critical crack length (formula defined below in subsection 2.3.3). The length represents the minimal crack length to start a super shear crack propagation*.

2.3.2. Slab depth and structure ratio

The goal of this section is to validate our simple planar slope simulation results with the long-bowl simulations. We present in *Figure 7* the results with different slab depths covering the structure with an initial density of 80 kg m^{-3}. The threshold to distinguish an arrest or a propagation is between 0.2 and 0.25 m (no intermediate values tested), which is approximately the same as reported in

Figure 5-a, with an initial density of 80 kg m^{-3}. The only values that resulted in a crack arrest are those with a structure ratio (height/width) of 0.5, resulting in a local steep angle at the structure for the crack to go above.

With our simulation set-up, we model the structure as a Gaussian ridge (smooth ridge) as presented in Figure 1-a. We control the width and the height of the structure; therefore, we could explore the sensitivity of these two parameters on the occurrence of crack arrest or propagation through the structure. *Figure 7* shows that the structure ratio is important at the threshold slab depth value covering the structure. The ratio acts here as a secondary variable compared to the slab depth covering the structure, where its influence is important only at the threshold value (depending on the initial density value).

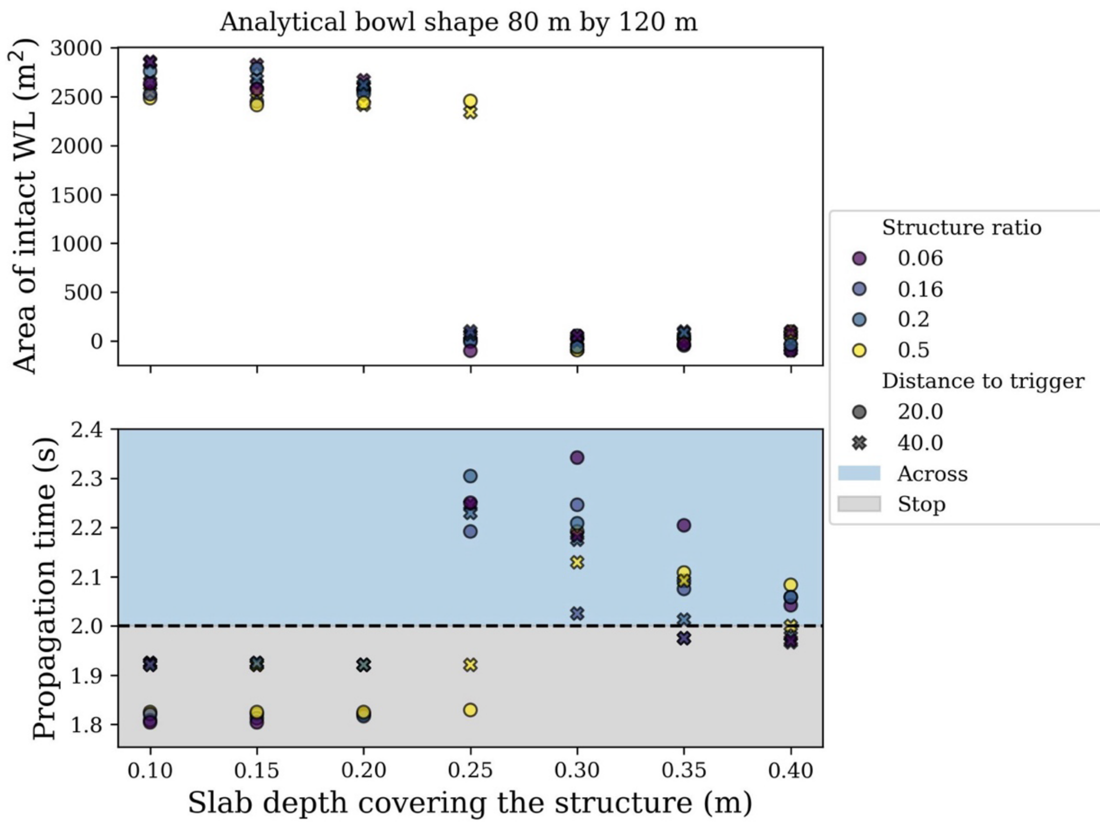

Figure 7. ***Long-bowl simulations.*** *Area of intact weak layer (top) and crack propagation time (bottom) versus slab depth covering a buried cross-slope structure for* $\rho_0 = 80$ *kg·m*$^{-3}$*. Colors indicate structure aspect ratio (*H_{wall}/W_{wall}*) and symbols the distance from the trigger. Crack arrest occurs below the critical slab depth (0.20–0.25 m) and only for the largest aspect ratio (*$H_{wall}/W_{wall} = 0.5$*), consistent with planar slope simulations. Slab depth is the primary control on propagation, while distance from the trigger has a limited influence within the tested range.*

The position of the structure relative to the trigger or a remote avalanche control system (RACS) is of great interest when planning avalanche mitigation structures. We tested different distances from the trigger in our long-bowl simulation, starting from the far left of the slope to approximately 5 m from the structure. Results suggest that the influence of the distance to the trigger is quite negligible, as there is a small influence for a specific value of the structure ratio, meaning that the distance from the trigger is less important than the structure ratio, which is also less important than the slab depth covering the structure (*Figure 7*).

Lay summary 2.3.2: Numerical simulations suggest that if the slab depth covering the structure is near 0.2 and 0.25 m, then the structure ratio between the height and the

width is important and should be at least 0.5 to prevent the propagation across the structure.

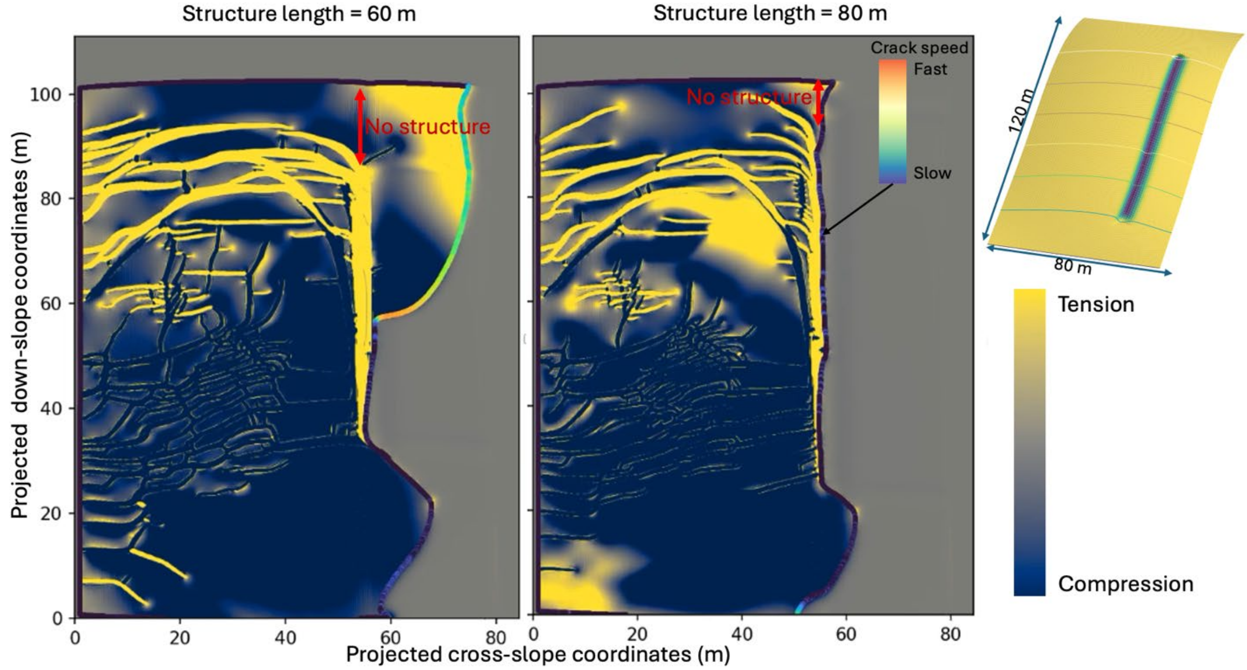

Figure 8. ***Top-view comparison of crack propagation for structure lengths of 60 m (left) and 80 m (right).*** *The shorter structure (60 m) fails to arrest the avalanche because the unprotected gap at the top of the slope (indicated by the red arrow) is large enough for the crack to bypass the barrier. The longer structure (80 m) successfully arrests the propagation by reducing this gap to a critical threshold where the crack cannot sustain itself. The color map represents the stress state of the slab, with yellow indicating tension and blue indicating compression. The color outline indicates the crack propagation speed.*

2.3.3. Structure length

With our long-bowl simulation, we tested different lengths in the down-slope direction for an ideal structure. *Figure 8* shows two simulations (top-view) with two different structure lengths. The left simulation shows a propagation that passes through the top part of the slope because the length where there is no structure is very important. The simulation on the right shows an arrest because this same length (no-structure) is reduced. The absence of structure in the upper section corresponds to a decrease in slope angle below the snow friction angle (27°), limiting the shear stress in the weak layer. More simulations were needed to find the ideal length that could distinguish between the arrest and the propagation. The ideal length depends on, once again, the slab depth covering the structure; thus, *Figure 9* shows that different lengths seem to distinguish an arrest from a propagation. For a H_{slab} of 0.3 m, the propagation occurs for every value of structure length. However, with a thinner slab, there is an arrest with a structure length of 65 m at 0.2 m H_{slab}, and 70 m with 0.25 m of H_{slab}. Respectively, the remaining length where there is no structure is 12 m for the 70 m structure length and 15 m for the 65 m structure. Thus, this length also corresponds to the slope where the angle is below the snow friction angle where it is less prone to promote crack propagation. For long structures (>70 m), the protected region spans most of the slope where the inclination exceeds the snow friction angle. For shorter structures, a portion of the slope with angles above this threshold remains unsupported, allowing shear-driven crack propagation to develop across the full slope. Lastly, the length corresponds approximately to the super shear critical crack length (a_{sc} around 5-7 m for θ around 30 °), which is the length of the damaged weak layer sufficient to promote crack propagation in shear mode (Gaume et al., 2013; Guillet et al., 2023), given by:

$$a_{sc} = \Lambda \left(1 - \frac{\tau_p}{\tau_g}\right) \frac{tan\theta}{tan\theta - tan\phi}$$

where Λ is the characteristic elastic length of system (snow properties) (Chiaia et al., 2008), τ_p is the weak layer shear strength, τ_g is the shear gravitational stress (slab weight), ϕ is the snow friction angle, and θ is the slope angle. The length corresponds to the length of the crack necessary to propagate, with tension in the slab above the slope. Similarly, the slab below the crack will be in compression. However, the length defined by a_{sc}, corresponds to the slab in tension above, so its need to be approximately $2a_{sc}$ to account for both compression (below) and tension (above) (Chiaia et al., 2008; Gaume et al., 2013). This crack length was determined for the release and on the onset of crack propagation in shear mode, but its seems that this length might also be important to the arrest as the "minimal gap" covers by the structure seems to be approximately equivalent.

<u>Lay summary 2.3.3</u>: The optimal structure length in the down-slope direction is where the slope angle is below the snow friction angle. If it is not possible, this distance between the structure and the location where the slope angle is below the snow friction angle should not be more than $2a_{sc}$, typically around 10-15 m for 30° slope angle.

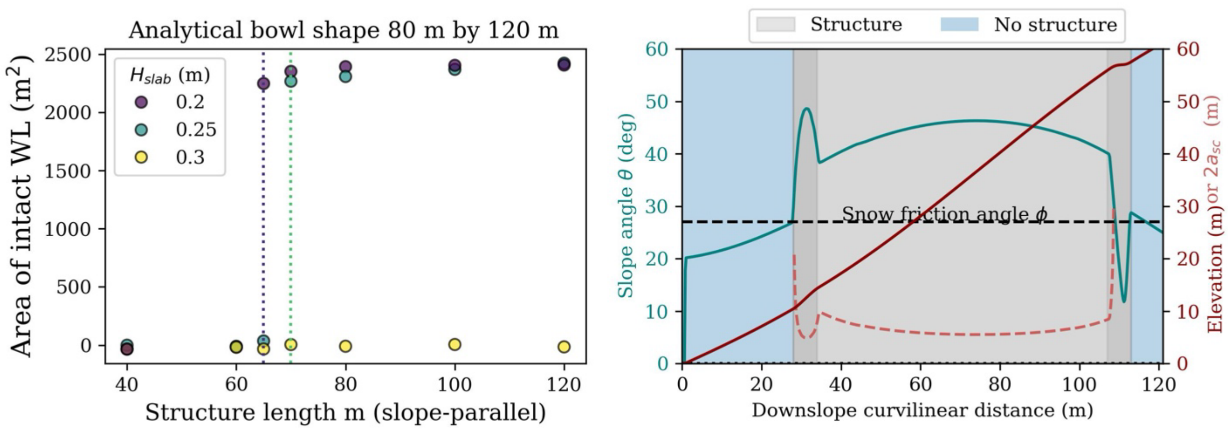

Figure 9. ***Influence of structure length on crack arrest. (a)*** *Intact weak layer area versus structure length for three slab depths (H_{slab}). A specific length threshold (65–70 m) is required to arrest cracks in thinner slabs (0.2 to 0.25 m), while thicker slabs (0.3 m) propagate regardless of structure length.* ***(b)*** *Downslope profile showing slope angle (teal) relative to the snow friction angle (dashed line). Effective arrest depends on minimizing the "gap" of unprotected steep terrain above the structure. If this gap exceeds the super shear critical crack length ($2a_{sc}$ approx 10 to 15 m), the crack gains enough energy to propagate around the structure.*

2.4. Long-bowl simulation with unburied structure

We tested a different type of **unburied** structure that is discontinuous along the downslope direction (Figure 2), consisting of one linear and two offset structures. This structure was originally thought to consist of rocks and trees that could generate enough heterogeneity to stop the propagation. First, we tested a simple linear discontinuous structure with different spacings and structure lengths. *Figure 10* demonstrates two simulations with a spacing of 8 m and 9 m; the other structural parameters are the same. The 8 m spaced structure was able to stop the crack propagation. The propagation went through the discontinuities (right) where the slope angle is at maximum (around 38°), at this angle, the $2a_{sc}$ is around 9 m, which is approximately the structure spacing at which propagation across occurs. It is important to keep in mind that $2a_{sc}$ is a combination of both terrain and snow properties, meaning that the 8-9 m of structure spacing (approximately $2a_{sc}$) is dependent the maximum slope angle, but also the slab (density and elastic modulus) and the weak layer properties (shear strength and stiffness). It is important to note here that the propagation in supershear propagation might stop but the anticrack propagation might continue at lower speed causing a delay in the propagation.

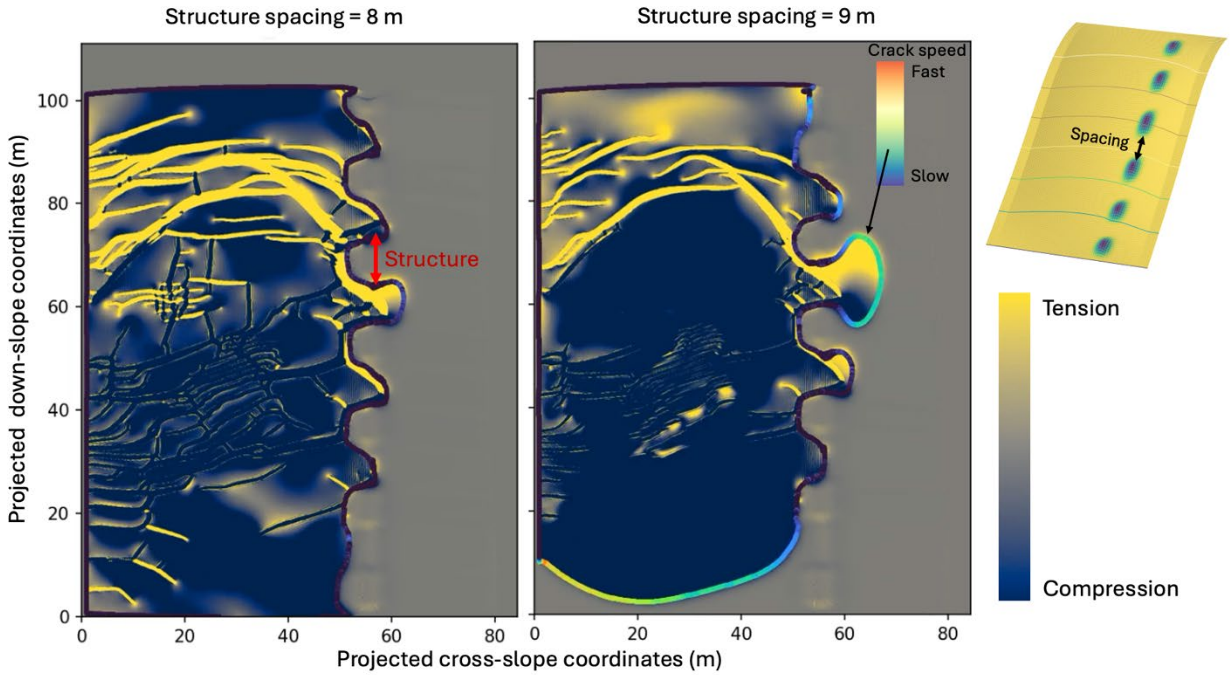

Figure 10. ***Top-view comparison of crack propagation for unburied discontinued structure with an 8 m spacing (left) and 9 m spacing (right).*** *The shorter spacing (8 m) successfully arrests the propagation by reducing this gap to a critical threshold where the crack cannot sustain itself. The longer spacing (9 m) fails to arrest the avalanche because the gap at the steepest part of the slope is large enough for the crack to bypass the barrier. The color map represents the stress state of the slab, with yellow indicating tension and blue indicating compression. The color outline indicates the crack propagation speed.*

We tested two offset **unburied** discontinued structures to see if the spacing could be higher if the two structures were offset. Multiple simulations were conducted with both the single and the two offset structures with different spacing configurations. *Figure 11* shows that the ideal spacing for one single discontinued structure is around 8 m, compared to the spacing from two offset structures, where only a spacing of 1 m could stop the propagation. It is important to note here that spacing are different in a sense that for the single structure, it is only a structure spacing in the downslope direction (y-axis) relating the closest structure, compared to the two offset structures where it's a distance in the x-y plane relating the closest structure (*Figure 11*). This result shows that it is more important to constrain crack propagation with a structure spacing in the down-slope direction (y-axis) than in the x-y direction.

Lay summary 2.4. Our analysis suggests that a linear single structure assembly is more efficient that two linear structure assembly with lateral offset. The spacing between the structure should be at minimum 8 m. However, anticrack propagation may continue instead of an arrest and cause a delay.

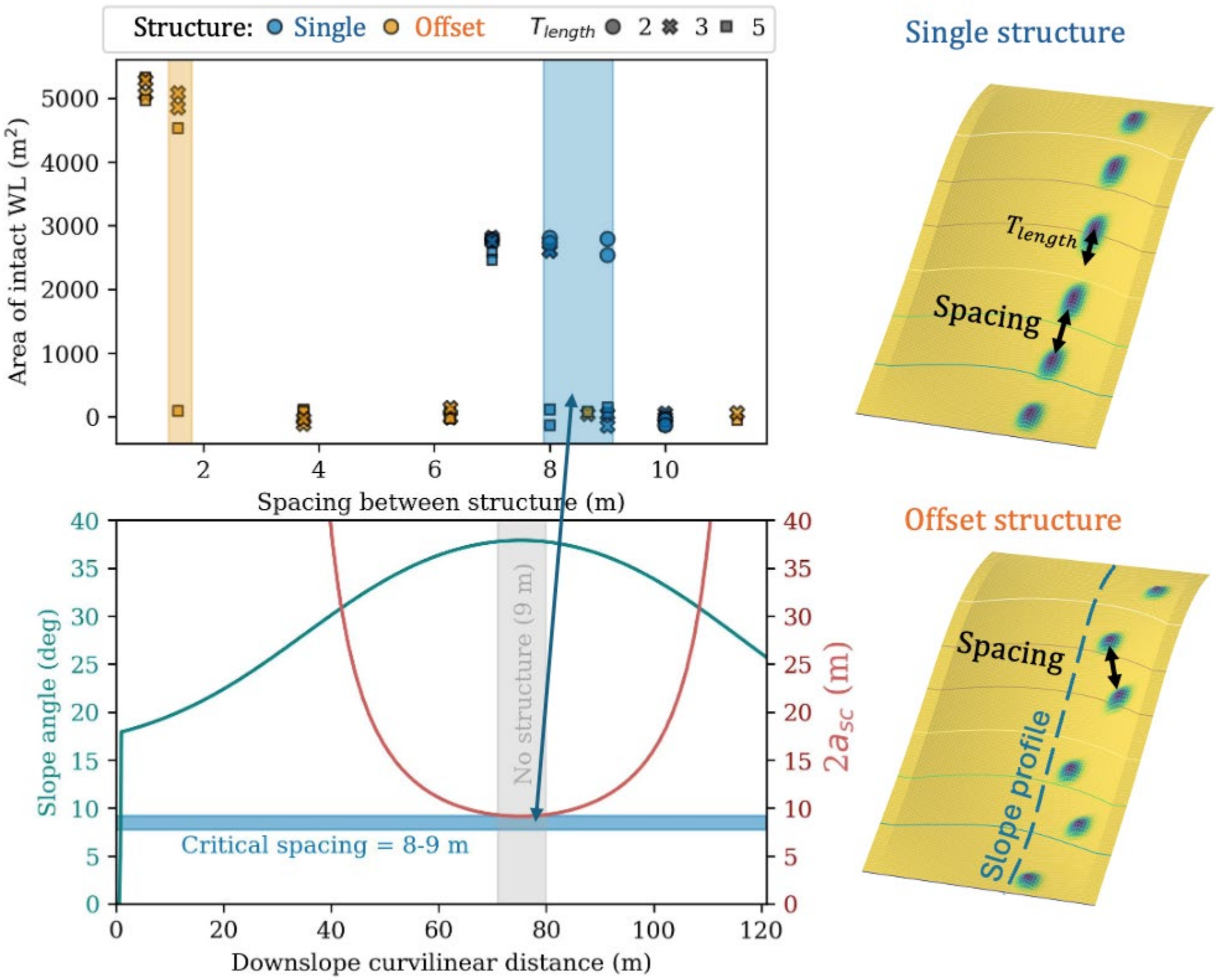

Figure 11 ***Sensitivity analysis of spacing for unburied discontinued structures, both single and two offset structures. (Top)*** *Results for a single linear row of structures and two offset rows of structures. The different symbols represent the Taper length of the structure T_{length} in the downslope direction (Figure 2). (Bottom) Crack arrest is achieved at a spacing of approximately 8-9 m for a linear single structure, which roughly corresponds to the double super shear critical crack length ($2a_{sc}$) on the steepest part of the slope. The spacing required for two offset rows of structures requires a much tighter spacing (approx. 1 m).* ***Comparison:*** *The results indicate that blocking propagation in the direct downslope direction (single row) is more effective than attempting to block it in the x-y plane (offset rows), as the crack can more easily navigate diagonal gaps.*

3. Case study for Stanley Path, Colorado

For this project, we adapted the DAMPM model code to operate on real-world complex topography, enabling crack-propagation simulations on a Digital Elevation Model (DEM). With a 1-m Lidar derived DEM, we were able to run simulations on the Stanley Path in Colorado, above CO Highway 40. The exposure to the highway is already quite well known, and Remote Avalanche Control Systems (RACS) were installed at multiple trigger locations in the starting zone of the Path (*Figure 1*-d). There are two GazEx (RACS) installed on the study slope, and the idea from the local forecaster and project investigator (Ron Simenhois) was to place the structure between the two GazEx positions. We simulate a ridge-like structure in addition to the DEM, so the structure will follow the terrain. To achieve realistic spatial variability of slab depth, we used the Winstral algorithm to simulate over the DEM, snow erosion, and snow accumulation areas with a predetermined wind direction (Winstral et al., 2002). We tested a wind direction that would replicate a cross-loaded slope, because the local forecaster (Ron Simenhois) has reported that this scenario tends to produce bigger avalanches. We then used the Winstral index to parameterize the slab depth to achieve a variation of approximately from 0.1 to 0.5 m across the slope. This parameterization can also provide an investigation into the crack propagation behavior over the structure that has been cross-loaded, and the slab depth accumulation is not symmetrical on the structure.

We show two different simulations with different slab depth minimums both overtopping the barrier. The simulation with the H_{slab} minimum is 0.15 m, shows that the crack propagation is being stopped at the structure. The arrest is possible due to slab fractures but also that less shear stress can sustain a shear crack propagation, due to less slab weight and local steep slope caused by the structure. The other simulations with a slightly thicker H_{slab} minimum (0.2 m) had a propagation across the structure, still with a slab tensile fracture occurring at the structure, but the shear stress was sufficient to sustain the crack propagation across the structure.

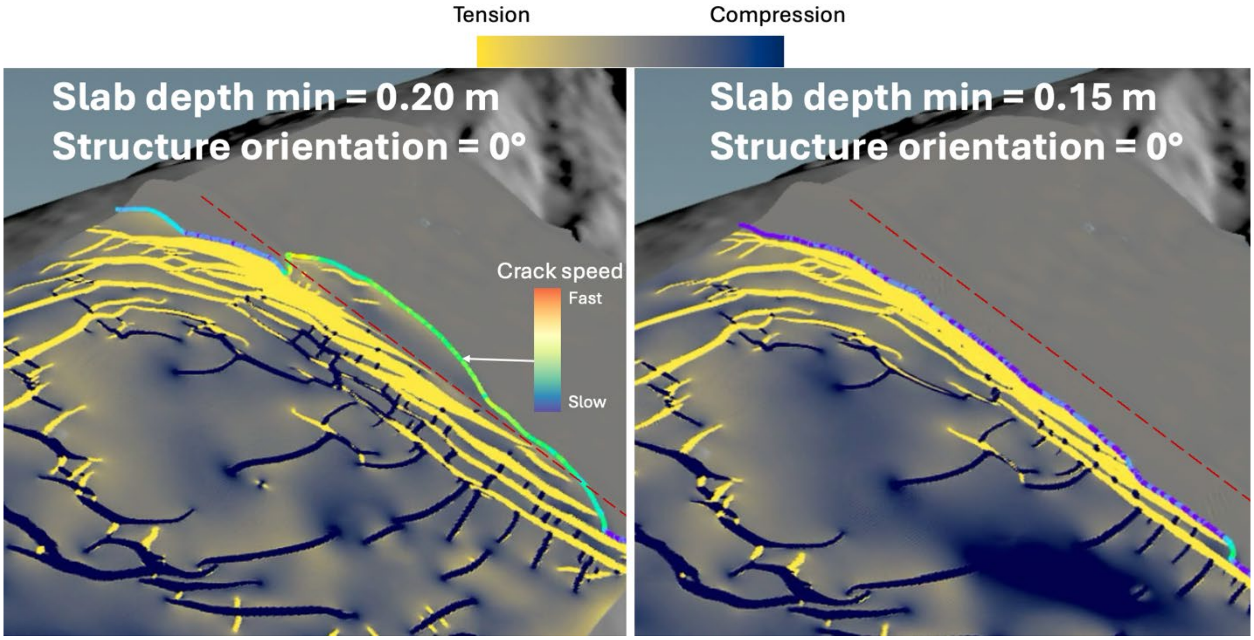

Figure 12. ***Stanley Path simulation with two different slab depth minimum and with a structure orientation of 0° (from the x-axis).*** *The blue-yellow color bar represents the tension and the compression stresses/fractures in the slab. The color outline represents the crack front and the crack speed.*

Lastly, we present a sensitivity analysis for several parameters to effectively plan a possible installation in the future. We tested different structure ratios, minimum slab depths covering the barrier, and the structure orientation in the starting zone. *Figure 13* shows all the simulations conducted for the Stanley Path. For the slab depth covering the slab, similar results were obtained compared to the simulations above (planar slope and long-bowl), where almost all the simulations were stopped with H_{slab} = 0.15 m, and a few simulations stopped at 0.2 m. Interestingly, the simulations (H_{slab} = 0.2 m) that have stopped at the structure are simulations with a structure ratio at or above 0.5, and the structure orientation above 10° (from the x-axis). The only simulation that resulted in an arrest with a thicker slab was with a structure ratio of 0.8 and an orientation of 20° (x-axis). However, the structure with a 20° orientation is very close to the trigger location and could affect this result. In addition, a 20° orientation shifts the structure toward a more cross-slope configuration, like a traditional snow fence, thereby deviating from the original concept of downslope-oriented structures.

Lay summary 3: For the Stanley Path, our results suggest similar results as in our previous simulations, namely a minimum slab depth covering the structure at 0.2 m (initial density of 80 $kg \cdot m^{-3}$) and a structure ratio of 0.5. In addition, we found the best structure orientation was 10° (x-axis), to effectively stop the crack propagation.

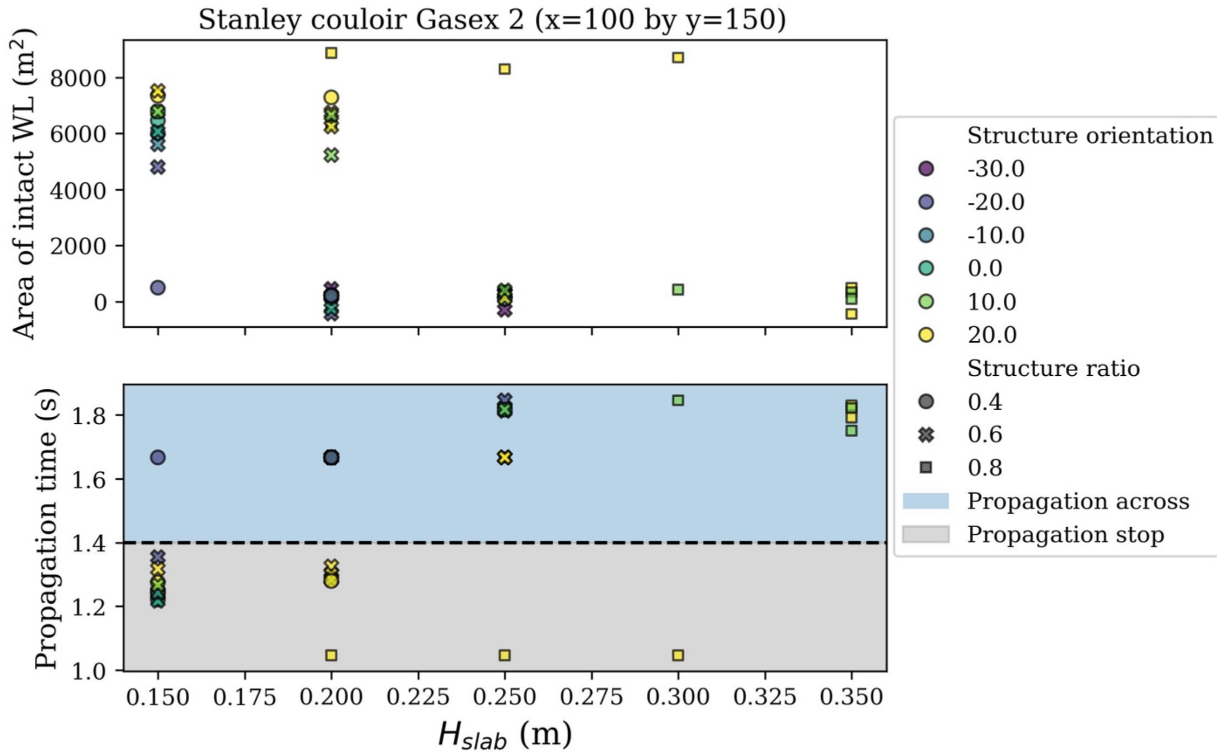

Figure 13. ***Sensitivity analysis of design parameters for the Stanley Path case study.*** *The plots show the area of the intact weak layer (top) and propagation time (bottom) as a function of slab depth (H_{slab}). Symbols distinguish the structure's aspect ratio (H_{wall}/W_{wall}) and the colors represent the structure orientation relative to the x-axis. Slab depth is the primary control on effectiveness, with most simulations successfully arresting the crack at H_{slab} = 0.15 m. For slightly thicker slabs (0.2 m), successful arrest depends on secondary factors: it requires a steeper structure (ratio >= 0.5) and an orientation greater than 10°.*

4. Summary and structural design recommendations

This work was an exploration through numerical modeling to test the feasibility of a down-slope structure that promotes crack arrest and limits avalanche release size during avalanche control activities. This section aims to summarise our results from all simulations presented in this report. For each type of simulation presented above in Table 2 and Table 3, we present below the key findings respectively in Table 4 and Table 5. From these key findings, we suggest some structural design recommendations and, lastly, present the next step towards a new type of mitigation structure.

The confidence in our results is good because the model that we used was validated with various experimental datasets (Bergfeld et al., 2025; Bobillier et al., 2024; Gaume et al., 2019; Trottet et al., 2022). This method was also used to improve our process-understanding regarding the initiation, the onset of propagation, and the dynamic crack propagation (crack speed regime). Some parts of the mechanism responsible for the arrest are still unknown and were beyond the scope of this study. For example, we still don't know to what extent the influence of the slab fracture promotes crack arrest during the super shear regime. From the results of Meloche et al. (2025), we know that there is an interplay between a relative decrease in crack speed, either by an increase in shear strength (WL strength) or a decrease in shear stress (slope angle), combined with slab fractures. However, we have not yet quantified what the necessary "slow down" of the crack speed is needed to stop the propagation with a slab fracture. From this project perspective, it is difficult to find a general rule to predict crack arrest based on all possible snow properties and structural dimensions that were not tested in our model. In addition, our model only reproduces shear-based propagation, which is valid for most of the cases presented in this report. However, it is possible that, instead of an arrest, the propagation regime goes to a collapse-based propagation, namely anticrack propagation, with much slower crack speed. We may say that there will be a strong reduction of crack speed and, therefore, higher potential for arrest through an increase in tensile stress (Meloche et al. 2025). If there is no arrest, we may still have a delay that could impact the overall avalanche release dimension. Thus, we can only make recommendations based on the simulations conducted during this project, which is still significant with 300 simulations and over 18 Tb of data.

4.1. Structure dimensions

In the case where there is no weak layer or the structure is unburied, the required width is relatively small, around 0.6 m, which is approximately the characteristic elastic length Λ (Table 4). Then, when the structure is buried, the effective width caused by the snow burial will increase, and from the tested width, the minimum width is linked to the structure height by the structure ratio. We found that the minimum structure ratio needed to cause an arrest was 0.5 (height/width) (*Table 5*). However, the most important parameter that distinguishes between an arrest and a propagation is the slab depth covering the structure, and this specific value depends on the initial density. If the density is low, the maximum slab depth covering the structure can be around 0.3 m compared to 0.15 m for a higher density (*Table 5*). Lower densities can be related to either a calm storm or a continental snowpack. Higher densities can be related to either a wind slab or a maritime snowpack.

This result suggests that the structure should be designed to emerge from the snowpack as much as possible to minimise snow covering the structure. Information about the typical snow depth or snow depth maps in potential release areas should be gathered to adequately estimate the snow depth. In addition, avalanche control should be conducted regularly to prevent snow from accumulating and covering the structure with as little as 0.3 m of snow above it. However, these relatively low values of slab depth covering the structure were obtained with a spatially homogeneous weak layer strength. As reported by many researchers (Gaume et al., 2013; Meloche et al., 2023; Reuter et al., 2016), a heterogeneous weak layer is more realistic and could promote crack arrest more easily. Thus, we can expect that thicker slab depth covering the structure will still cause crack arrest when using a heterogeneous weak layer (more realistic).

Table 4. Key results for the simulation ***with no weak layer or unburied structure*** *with the parameters listed in Table 2.*

No weak layer or Unburied structure			
Parameters/Simulation	Planar slope 30 by 10 m	Long bowl 80 by 120 m	Discontinued structure 80 by 120 m
Key objectives of the simulation	Minimum width wall with no slab on top.	Minimum width with slab on top, but no weak layer.	Minimum spacing between structure.
Main Results	**Wall width minimum of around 0.6 m**	**Wall width minimum of around 0.6 m**	**Minimum spacing of $2a_{sc}$ around 8-9 m**
Results presentation	Section 2.1 Figure 3	Section 2.3.1 Figure 6	Section 2.4 Figure 10-11

The width of the structure needs to be determined primarily in relation to the ideal height mentioned previously, to respect the structure ratio above 0.5 (ideally), height over width, assuming a triangular shape. Even though the structure ratio is a secondary variable, our results show that it can promote crack arrest when the slab depth value is at the threshold value between arrest and propagation (around 0.25 m, depending on the initial density).

4.2. Layout in the starting zone

Our results show that the down-slope length can be effectively planned using a digital elevation model and the slope angle. *Figure 9* shows that the smallest length at which an arrest occurs is around 70 m; the structure ends approximately where the slope angle is at 27° and below (the snow friction angle). Below this angle, shear propagation cannot be sustained; therefore, we obtained an arrest. The length for a potential structure can be estimated using a digital elevation model and the slope angle. For example, starting from a ridgeline (around 0°), the length of the structure should start around 27°.

The orientation in the starting zone was tested in the Stanley Path starting zone. Different orientations were tested from 20° to -30° (x-axis), providing enough values from almost cross-slope orientation, like snow fencing (20° x-axis), to down slope orientation (around -10°). Our results indicate that 20° was the best orientation to cause an arrest. However, with that orientation, the structure was relatively close to the trigger (GazEx 2), and the orientation was near the cross-slope structure, like a snow fence. When the orientation is slightly lower, around 10° to 0°, there is no propagation with a lower slab depth covering the structure (0.2 m instead of 0.25 to 0.3 m) and a structure ratio above 0.5. Lastly, when the orientation is around -10° to -20°, the slab depth covering the structure needs to be lower, around 0.15 m, to promote crack arrest.

*Table 5. Key results for the simulation **with weak layer or buried structure** with the parameters listed in Table 3.*

Buried structure **(with weak layer)**				
Variables	Planar slope 30 by 10 m	Long bowl 80 by 120 m	Long bowl 80 by 120 m	Stanley Path 100 by 150 m
Key objectives of the simulation	Minimum slab depth covering the structure and initial density.	Minimum slab depth covering the structure (bigger slope).	Minimum length of the structure.	Minimum slab depth and structure orientation.
Main Results	H_{slab} **threshold values from 0.2 to 0.3 depending on initial density** ρ_0	$\boldsymbol{H_{slab}}$ **threshold values from 0.25 for** ρ_0 **= 80 kg m**$^{-3}$ **and structure ratio of 0.5 (height/width)**	**65-70 m structure length where slope angle is above snow friction angle**	$\boldsymbol{H_{slab}}$ **threshold values from 0.2 for** ρ_0 **= 80 kg m**$^{-3}$**, structure ratio of 0.5 (height/width), and orientation of 10°**
Results presentation	Section 2.1 Figure 4-5	Section 2.3.2 Figure 7	Section 2.3.3 Figure 8-9	Section 3 Figure 12-13

4.3. Delays in crack propagation

It could be of interest to introduce a significant delay in crack propagation, as this could lead to the formation of two smaller avalanches and thereby limit the final release size. In the simulations, we measured the total crack propagation time for both the long-bowl (*Figure 7*) and Stanley Path configurations (*Figure 13*). We observed that the presence of the structure induces a delay of approximately 0.3–0.5 seconds. However, this delay is too small to generate two distinct avalanches, and therefore insufficient to significantly limit the extent of crack propagation. There is a possibility that delays could be more significant if, instead of an arrest, the propagation speed slows down significantly to the anticrack collapse-based regime (approx. 40 m/s) and crosses the structure at a much lower speed than the shear-based regime in the cross-slope direction in mode III (approx. 100-80 m/s).). Then, delays should be more important (1 seconds) and might cause two avalanches instead of one. Unfortunately, we could not observe this slow-down to the anticrack regime, as our model is only able to assess the shear-based propagation and could not reproduce this collapse-based propagation. From a practical standpoint, delays could be expected with this type of cross-slope structure; however, they should still be in the order of 1 seconds, which are still relatively small delays.

4.4. Next step

Based on our results, we are confident that down-slope structures designed to promote crack arrest or reduce avalanche size have clear potential and warrant further investigation. The next step towards implementing a new type of mitigation structure is to conduct a new phase of research and potential testing. This second phase should focus mainly on optimising a design that could resist significant snow burial and wind loading, involving a geotechnical engineer who specialises in geotechnical structures in alpine environments. We believe that through this first phase; we uncovered the main guidelines of the structure regarding snow mechanics and the feasibility of a down-slope structure promoting crack arrest. With these guidelines in mind, the next phase should focus on designing a structure that will emerge from the snow cover, resist heavy wind loading, and bear the stress of a thick snow cover throughout multiple winters. As mentioned previously, our model cannot actively simulate the burial of the structure by snow, as it can only reproduce the slab, the weak layer, and the terrain directly underneath. This simple representation would not affect the results of crack propagation, as the structure was modelled as a "smooth gaussian ridge," which likely reproduces a progressive "smoothing" during the snow burial of the structure. Then, if necessary, an additional round of numerical simulations could be performed with these specific designs to validate their efficiency in terms of snow mechanics and crack propagation.

4.5. Field experiment and site

The possible field site for testing should be the Stanley path in Colorado, as preliminary simulations were done using the terrain. Preliminary structural design could be tested at this location, such as earth-structures (gabians) or metal stand-alone structures. In terms of snow mechanics and crack propagation, the decision between these types of structures is not relevant as long as they respect the geometry requirements (structure ratio) above 0.5. Thus, the decision on which types of structures to install should consider their ability to resist snow accumulation throughout the winter and the logistics of installing such structures in an alpine terrain.

An AI generated structure is proposed based on the different results obtained from this study in Figure 14. The structure is relatively lightweight and could dissipate the slab induced stress during crack propagation, by having two separated light walls. This space in between would allow for the minimum width from our simulations (

Figure 5-Figure 6), while keeping the structure relatively light with less material in comparison to one wide structure.

Figure 14. An AI-generated conceptual illustration of a lightweight structure designed to arrest weak-layer crack propagation by absorbing slab-induced stresses and preventing their transmission from one side of the structure to the other.

The structure width could be based on the values obtained from the “no weak layer” and unburied simulations (*Table 4- Figure 3 - Figure 6*), reporting widths on the order of 1 m. However, when the structure becomes buried, the “effective width” that we model as smooth Gaussian will increase due to snow accumulation around the structure, thereby decreasing the height-to-width ratio. As shown by the simulations, maintaining a ratio above 0.5 is critical, with a structure height comparable to the average snow depth at the study site. Such structures will likely modify local wind fields, generating erosion and deposition patterns that were not previously present. Wind-driven snow accumulation around the structure may further increase burial and effective width. Recent snow distribution models now allow fully three-dimensional wind-field simulations around structures, enabling realistic representation of snow accumulation around buildings (Hames et al., 2025) and alpine solar farms (Frischholz et al., 2026). The next research phase should therefore focus on a targeted structural design that explicitly accounts for snow burial and wind effects, combined with field deployment of a prototype to experimentally evaluate performance based on the recommendations of this report.

<u>Final lay summary</u>: The next phase should focus on an efficient design to resist snow accumulation and wind redistribution while respecting the dimensional recommendations in Table 4 and Table 5.

5. References

Chiaia, B. M., Cornetti, P., & Frigo, B. (2008). Triggering of dry snow slab avalanches: stress versus fracture mechanical approach. *Cold Regions Science and Technology*, *53*(2), 170–178. https://doi.org/10.1016/j.coldregions.2007.08.003

Frischholz, Y., Hames, O., & Lehning, M. (2026). Optimizing snow distribution in alpine PV systems: CFD-based design guidelines for power plant layout. *Cold Regions Science and Technology*, *241*, 104654. https://doi.org/10.1016/j.coldregions.2025.104654

Gaume, J., Chambon, G., Eckert, N., & Naaim, M. (2013). Influence of weak-layer heterogeneity on snow slab avalanche release: Application to the evaluation of avalanche release depths. *Journal of Glaciology*, *59*(215), 423–437. https://doi.org/10.3189/2013JoG12J161

Gaume, J., Schweizer, J., Herwijnen, A., Chambon, G., Reuter, B., Eckert, N., & Naaim, M. (2014). Evaluation of slope stability with respect to snowpack spatial variability. *Journal of Geophysical Research: Earth Surface*, *119*(9), 1783–1799. https://doi.org/10.1002/2014jf003193

Guillet, L., Blatny, L., Trottet, B., Steffen, D., & Gaume, J. (2023). A Depth-Averaged Material Point Method for Shallow Landslides: Applications to Snow Slab Avalanche Release. *Journal of Geophysical Research: Earth Surface*, 1–28. https://doi.org/10.1029/2023JF007092

Hames, O., Jafari, M., Köhler, P., Haas, C., & Lehning, M. (2025). Governing Processes of Structure-Borne Snowdrifts: A Case Study at Neumayer Station III. *Journal of Geophysical Research: Earth Surface*, *130*(3). https://doi.org/10.1029/2024JF008180

Heierli, J., Gumbsch, P., & Zaiser, M. (2008). Anticrack nucleation as triggering mechanism for snow slab avalanches. *Science*, *321*(5886), 240–243. https://doi.org/10.1126/science.1153948

McClung D., & Schaerer P. (2006). *The Avalanche Hanbook*. The Mountaineers Books.

Meloche, F., Bobillier, G., Guillet, L., Gauthier, F., Langlois, A., & Gaume, J. (2025). Modeling Crack Arrest in Snow Slab Avalanches—Toward Estimating Avalanche Release Sizes. *Journal of Geophysical Research: Earth Surface*, *130*(12). https://doi.org/10.1029/2025JF008470

Schweizer, J., Jamieson, J. B., & Schneebeli, M. (2003). Snow avalanche formation. *Reviews of Geophysics*, *41*(4), 3–5. https://doi.org/10.1029/2002RG000123

Sigrist, C., & Schweizer, J. (2007). Critical energy release rates of weak snowpack layers determined in field experiments. *Geophysical Research Letters*, *34*(3). https://doi.org/10.1029/2006GL028576

Trottet, B., Simenhois, R., Bobillier, G., Bergfeld, B., van Herwijnen, A., Jiang, C., & Gaume, J. (2022). Transition from sub-Rayleigh anticrack to supershear crack propagation in snow avalanches. *Nature Physics*, *18*(9), 1094–1098. https://doi.org/10.1038/s41567-022-01662-4

Winstral, A., Elder, K., & Davis, R. E. (2002). Spatial snow modeling of wind-redistributed snow using terrain-based parameters. *Journal of Hydrometeorology*, *3*(5), 524–538. https://doi.org/10.1175/1525-7541(2002)003<0524:SSMOWR>2.0.CO;2